Electronic Supplementary Material (ESI) for Physical Chemistry Chemical Physics.

Supplementary Information

Effects and Distribution of Zr Introduced in Ni-based Cathode Material for Li-ion Batteries

*Yongseon Kim**

Department of Materials Science and Engineering, Inha University, Incheon, 22212, Republic of Korea

AUTHOR INFORMATION

*E-mail: ys.kim@inha.ac.kr

S1. Determination of O_2 chemical potential for DFT calculation

It was reported that calculating the energy of O_2 molecules by the density functional theory (DFT) method provides incorrect values because of errors related to overestimation of the binding energies of the O_2 molecule and the electron added to O_2 when O^{2-} is formed.(S1) Therefore, the standard state chemical potential of O_2 is determined in a semi-empirical way to minimize the difference in the standard formation Gibbs free energy of metal oxides between the experiments and DFT calculations,(S2,S3) as expressed in the following equations, where the subscripts "C" and "E" denote computationally and experimentally obtained values, respectively.

$$G^{o}_{f_C}(NiO) = G^{o}{}_{C}(NiO) - G^{o}{}_{C}(Ni) - \frac{1}{2}\mu^{o}{}_{C}(O_2) \equiv G^{o}_{f_E}(NiO)$$

$$\rightarrow \mu^{o}{}_{C}(O_2) = 2\left\{G^{o}{}_{C}(NiO) - G^{o}{}_{C}(Ni) - G^{o}_{f_E}(NiO)\right\} \quad (S1)$$

$$G^{o}_{f_C}(ZrO_2) = G^{o}{}_{C}(ZrO_2) - G^{o}{}_{C}(Zr) - \mu^{o}{}_{C}(O_2) \equiv G^{o}_{f_E}(ZrO_2)$$

$$\rightarrow \mu^{o}{}_{C}(O_2) = G^{o}{}_{C}(ZrO_2) - G^{o}{}_{C}(Zr) - G^{o}_{f_E}(ZrO_2) \quad (S2)$$

From equation (S1), $\mu^{o}{}_{C}(O_2)$ is determined to be −14.834 eV when the Perdew–Burke–Ernzerhof projector-augmented wave (PAW_PBE) types of Ni, O, and Zr_sv pseudopotentials and the HSE06 hybrid functional are used, as implemented in the VASP code. This value yields only 0.13% error when applied to the ZrO_2 case (equation (S2)), showing excellent accuracy applicable for the Ni–Zr–O system. $G^{o}{}_{C}$ is approximated by energy values obtained from DFT calculations, which does not cause significant error, as reported by Ong et al.(S4)

S2. Surface energy of (012) obtained from differently sized crystal models

As discussed in section 3.1 of the paper, Zr doping in the LNO surface crystal model breaks the mirror symmetry of the model, which generates a polarity including an unwanted increase of the crystal energy. To prevent this error, Zr is located in the middle of the crystal blocks, as presented in Figure S1 (this figure is also

presented in Figure 3 of the main paper). However, this method requires changing the size of crystal models. For the bulk crystals, the size effect may be slight if the number of *k*-points is properly modified, because the DFT calculation is performed with periodic boundary conditions, but the surface models contain both the bulk crystal region and the surfaces. Therefore, it should be confirmed that the DFT calculation is not affected by the model size change. We calculated the surface energy of (012) and (003) planes with differently sized LNO models using the following equation:

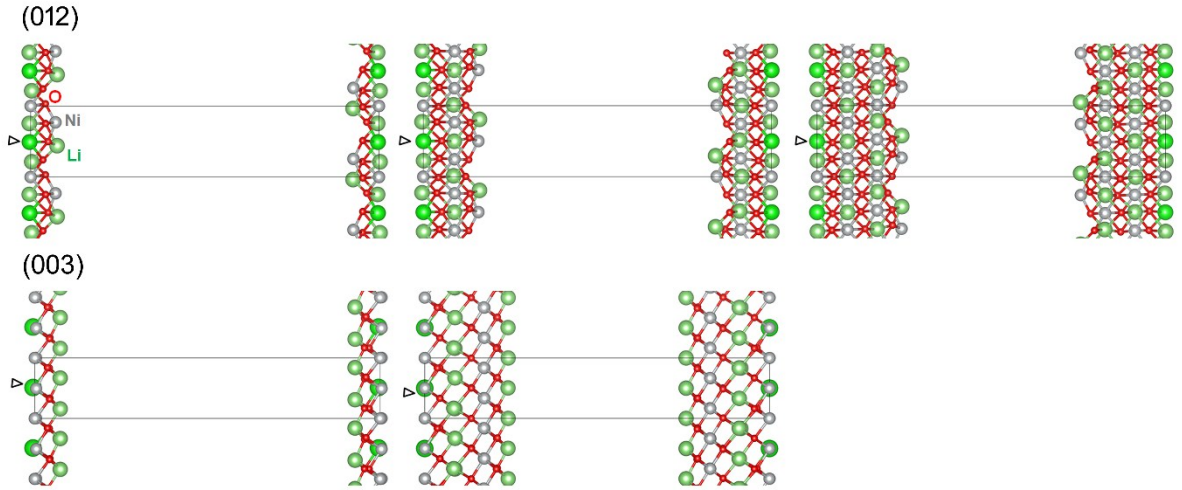

Figure S1. *Different sizes of surface crystal models for the DFT calculations: (upper) crystal models for (012) surface, and (lower) models for (003) surface. The doping position of Zr is marked with triangles.*

$$E_{surface\ model} \equiv E_{bulk} + 2E_{surface}$$

$$E_{surface} = \frac{1}{2}\left(E_{surface\ model} - E_{bulk}\right) \quad (S3)$$

In the above equations, $E_{surface\ model}$ is the energy of the model that includes the bulk crystal region and two surfaces at both sides of the crystal block; thus, the surface energy ($E_{surface}$) is calculated by equation (S3). The energy of the bulk crystal (E_{bulk}) is calculated from bulk crystal models with the same number of atoms as the surface crystal models. The calculation results are presented in Table S1, which shows similar values of the surface energy, indicating that changes in the sizes of the surface crystal models do not cause

significant calculation error.

Table S1. *Surface energy calculated from differently sized surface crystal models.*

Surface planes	Surface energy calculated from different size of models (eV/Å^2)		
(012)	0.1263	0.1238	0.1311
(003)	0.0611	0.0630	-

S3. Derivation of Equation (6)

It may be considered that the macroscale surface of Zr-doped LNO is a combination of Zr-doped and undoped surface crystal model units. The mixing of two kinds of crystal models can be driven by mixing entropy. If the equilibrium mixing ratio is calculated, then the concentration of Zr-doped units in the entire surface can be calculated, for which Equation (6) is used in the main paper. The equation is derived as follows:

$$\delta G = \delta G_{f,CM_{doped}} + \delta G_{mix} \approx G_{CM_{doped}} \delta N_{CM_{doped}} + \left(H_{mix} - TS_{mix}\right)\delta N_{CM_{doped}} \quad \text{(S4)}$$

$$\left(where \quad G_{CM_{doped}} \equiv \frac{\partial G_{f,CM_{doped}}}{\partial N_{CM_{doped}}},\ S_{mix} \equiv \frac{\partial S_{mix}}{\partial N_{CM_{doped}}} \approx -k \ln N_{CM_{doped}} \right)$$

$$\delta G \cong G_{CM_{doped}} \delta N_{CM_{doped}} + kT \ln N_{CM_{doped}} \delta N_{CM_{doped}}$$

$$\rightarrow \quad N_{CM_{doped}}^{eq} = \exp\left(-\frac{G_{CM_{doped}}}{kT}\right) \quad \text{(S5)}$$

where δG is the change in the Gibbs free energy that arises when a small amount of a crystal unit containing Zr is formed and mixed with undoped crystal units. The subscripts "f," "CM_{doped}," and "mix" in equation (S4) represent formation, doped crystal model, and mixing, respectively. By developing the equation, equation (S5), which is the final equation for the calculation of the equilibrium concentration of doped crystal units, is

obtained. The Gibbs free energy is approximated by the energy value obtained from DFT calculations for solid phases.

S4. Calculation of the diffusion length of Zr

The diffusion length of an impurity atom between lattice points can be expressed by the multiplication of the vacancy concentration, jump frequency, and the jump distance per unit movement.[S5] The jump frequency can be obtained from the lattice vibration frequency and the probability of an activated complex, that is, a state wherein the impurity atom is located at the saddle point of the diffusion route. Thus, the equation for the calculation of diffusion length is given as:

$$d \approx N_V \cdot \nu \cdot \exp\left(-\frac{E_b}{kT}\right) \quad (S6)$$

where N_V, ν, and E_b denote the vacancy concentration, lattice vibration frequency, and the diffusion energy barrier, respectively. Assuming the temperature of 1000 K and vacancy concentration of 1 ppm, the diffusion length d is calculated as ~4 μm in one hour in the [012] direction, whereas the length is only ~0.004 Å in the [003] direction, with the energy barriers of 1.35 eV to [012] and 2.70 eV to [003]. Although the length may change with temperature and vacancy concentration, the rough calculation shows much higher diffusion kinetics in the [012] direction compared to that for [003].

S5. Calculation of Zr distribution between Ni and Li sites

The distribution of Zr among the Ni and Li sites in the bulk LNO crystal can be quantitatively assessed by equation (11) in the main paper. The calculation results for the stoichiometric, Li-deficient, and delithiated LNO crystals are presented in the following Tables.

Table S2-S4*. Calculation results of the probability of Zr location at Li sites (P_n) in the LNO crystal of stoichiometric, Li-deficient, and delithiated states. The ten most probable crystal models determined by the CALYPSO code are shown in each table, and the partition function is composed with these 10 models. The*

crystal models in which Zr is located at Li site are tagged with "Zr_{Li}".

n	E_n-E_1 (eV)	25 ℃ (298 K)		400 ℃ (673 K)		600 ℃ (873 K)		800 ℃ (1073 K)	
		$e^{-\frac{E_n-E_1}{kT}}$	P_n	$e^{-\frac{E_n-E_1}{kT}}$	P_n	$e^{-\frac{E_n-E_1}{kT}}$	P_n	$e^{-\frac{E_n-E_1}{kT}}$	P_n
1	0.0000	1.000E+00	5.513E-01	1.000E+00	3.969E-01	1.000E+00	3.631E-01	1.000E+00	3.403E-01
2	0.0145	5.686E-01	3.134E-01	7.788E-01	3.091E-01	8.247E-01	2.994E-01	8.549E-01	2.909E-01
3	0.0407	2.051E-01	1.131E-01	4.959E-01	1.968E-01	5.823E-01	2.114E-01	6.441E-01	2.192E-01
4	0.0825	4.028E-02	2.221E-02	2.412E-01	9.573E-02	3.341E-01	1.213E-01	4.098E-01	1.395E-01
5	0.3264	3.024E-06	1.667E-06	3.598E-03	1.428E-03	1.306E-02	4.742E-03	2.932E-02	9.976E-03
6	0.6824	2.882E-12	1.589E-12	7.763E-06	3.081E-06	1.150E-04	4.175E-05	6.237E-04	2.122E-04
7	0.8351	7.544E-15	4.159E-15	5.581E-07	2.215E-07	1.511E-05	5.486E-06	1.196E-04	4.071E-05
8	0.9328	1.675E-16	9.233E-17	1.034E-07	4.104E-08	4.119E-06	1.496E-06	4.155E-05	1.414E-05
9_Zr_{Li}	1.2524	6.608E-22	**3.643E-22**	4.185E-10	**1.661E-10**	5.891E-08	**2.139E-08**	1.312E-06	**4.463E-07**
10	1.5191	2.035E-26	1.122E-26	4.208E-12	1.670E-12	1.699E-09	6.169E-10	7.325E-08	2.493E-08
Sum (Q)	-	1.814E+00	-	2.519E+00	-	2.754E+00	-	2.939E+00	-

n	E_n-E_1(eV)	25 ℃ (298 K)		400 ℃ (673 K)		600 ℃ (873 K)		800 ℃ (1073 K)	
		$e^{-\frac{E_n-E_1}{kT}}$	P_n	$e^{-\frac{E_n-E_1}{kT}}$	P_n	$e^{-\frac{E_n-E_1}{kT}}$	P_n	$e^{-\frac{E_n-E_1}{kT}}$	P_n
1	0.0000	1.000E+00	1.000E+00	1.000E+00	9.898E-01	1.000E+00	9.669E-01	1.000E+00	9.307E-01
2_Zr_{Li}	0.2826	1.660E-05	**1.660E-05**	7.647E-03	**7.570E-03**	2.336E-02	**2.258E-02**	4.704E-02	**4.378E-02**
3	0.3466	1.373E-06	1.373E-06	2.536E-03	2.510E-03	9.974E-03	9.644E-03	2.354E-02	2.191E-02
4	0.5696	2.327E-10	2.327E-10	5.426E-05	5.371E-05	5.148E-04	4.978E-04	2.112E-03	1.965E-03
5_Zr_{Li}	0.5916	9.871E-11	**9.870E-11**	3.712E-05	**3.674E-05**	3.842E-04	**3.715E-04**	1.664E-03	**1.549E-03**
6	0.8761	1.524E-15	1.524E-15	2.749E-07	2.721E-07	8.754E-06	8.464E-06	7.673E-05	7.141E-05
7	0.9895	1.845E-17	1.845E-17	3.893E-08	3.854E-08	1.940E-06	1.876E-06	2.252E-05	2.096E-05
8	1.7718	1.085E-30	1.085E-30	5.393E-14	5.338E-14	5.909E-11	5.713E-11	4.765E-09	4.434E-09
9	2.0279	5.052E-35	5.052E-35	6.512E-16	6.446E-16	1.963E-12	1.898E-12	2.985E-10	2.778E-10
10	3.6793	5.977E-63	5.977E-63	2.804E-28	2.776E-28	5.753E-22	5.563E-22	5.235E-18	4.872E-18
Sum (Q)	-	1.000E+00	-	1.010E+00	-	1.034E+00	-	1.074E+00	-

n	E_n-E_1(eV)	25 ℃ (298 K)		400 ℃ (673 K)		600 ℃ (873 K)		800 ℃ (1073 K)	
		$e^{-\frac{E_n-E_1}{kT}}$	P_n	$e^{-\frac{E_n-E_1}{kT}}$	P_n	$e^{-\frac{E_n-E_1}{kT}}$	P_n	$e^{-\frac{E_n-E_1}{kT}}$	P_n

1_Zr_{Li}	0.0000	1.000E+00	**1.000E+00**	1.000E+00	**9.999E-01**	1.000E+00	**9.987E-01**	1.000E+00	**9.944E-01**
2_Zr_{Li}	0.5709	2.217E-10	**2.217E-10**	5.311E-05	**5.310E-05**	5.064E-04	**5.058E-04**	2.083E-03	**2.072E-03**
3_Zr_{Li}	0.5860	1.228E-10	**1.228E-10**	4.088E-05	**4.087E-05**	4.139E-04	**4.133E-04**	1.768E-03	**1.758E-03**
4_Zr_{Li}	0.5875	1.159E-10	**1.159E-10**	3.986E-05	**3.985E-05**	4.059E-04	**4.053E-04**	1.740E-03	**1.730E-03**
5	1.2629	4.389E-22	4.389E-22	3.491E-10	3.491E-10	5.123E-08	5.116E-08	1.171E-06	1.164E-06
6	1.3305	3.151E-23	3.151E-23	1.088E-10	1.087E-10	2.085E-08	2.082E-08	5.633E-07	5.601E-07
7	1.5883	1.379E-27	1.379E-27	1.277E-12	1.277E-12	6.778E-10	6.769E-10	3.468E-08	3.449E-08
8	1.7691	1.204E-30	1.204E-30	5.647E-14	5.646E-14	6.122E-11	6.114E-11	4.904E-09	4.877E-09
9	2.9074	6.766E-50	6.766E-50	1.690E-22	1.690E-22	1.644E-17	1.642E-17	2.210E-14	2.197E-14
10	3.9891	3.443E-68	3.443E-68	1.342E-30	1.342E-30	9.362E-24	9.350E-24	1.836E-19	1.825E-19
Sum (Q)	-	1.000E+00	-	1.000E+00	-	1.001E+00	-	1.006E+00	-

S6. Examination of the strain–energy relation

The change of crystal energy of LNO under strain in the [012] and [003] directions is calculated by the DFT method. Two types of bulk crystal models, one for [012] and the other for [003], were prepared. After pre-optimization of the structures, different values of strain were applied in the [012] and [003] directions by changing the length of the lattice vector in these directions in each model crystal; the structures were then optimized again. The lengths of the lattice vectors in the [012] and [003] directions were fixed at the changed value, while those of other two lattice vectors and the atomic positions in the crystal were allowed to change during the second structural optimization. We used the QUANTUM-ESPRESSO code instead of VASP, which can allow only a part of the lattice parameters to change during the structure optimization process. The strain–energy relations for the [012] and [003] directions are thus obtained as presented in Figure S2, which indicates that the LNO crystal is easier to elongate in the [012] direction than in the [003] direction.

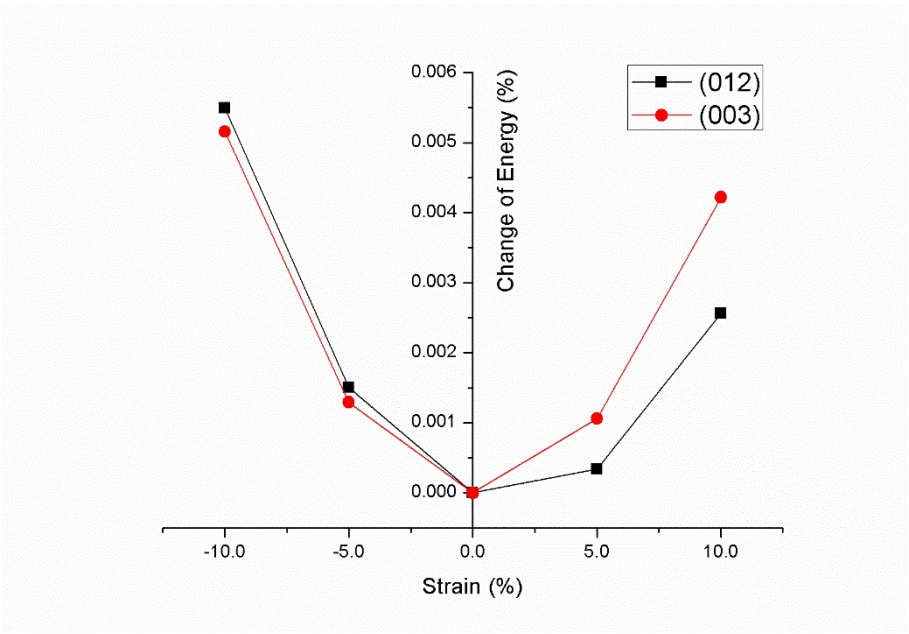

Figure S2. *Strain–energy relations of LNO obtained from DFT calculation.*

S7. Density of states (DOS) before and after Zr doping

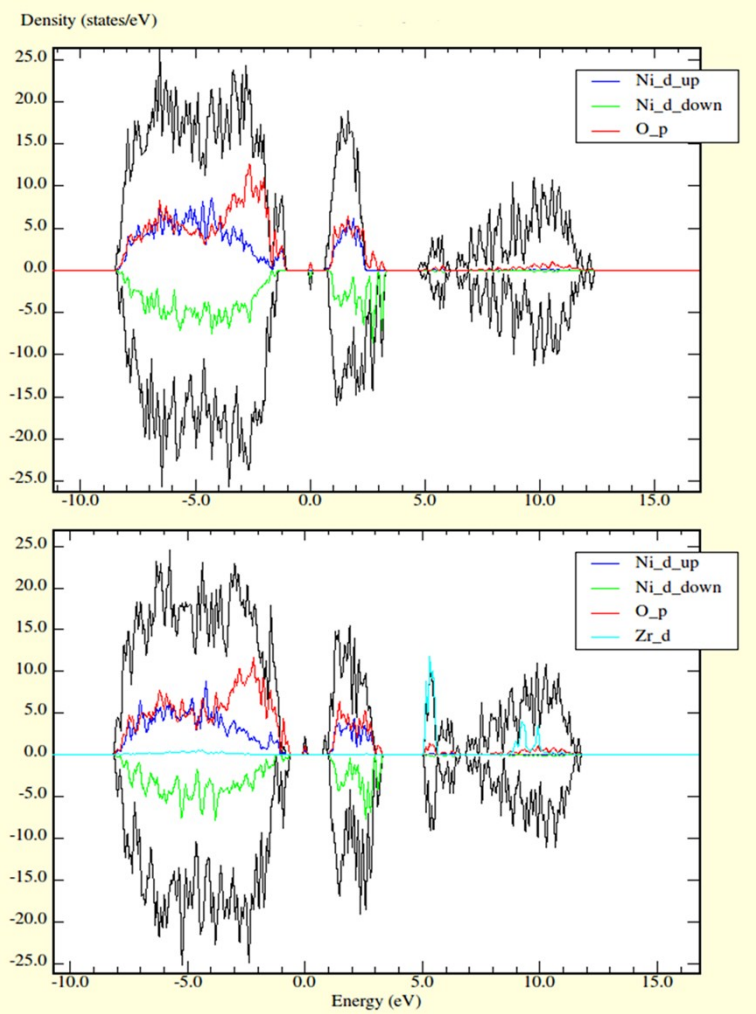

Figure S3. *Density of states (DOS) diagrams of surface crystal model of LNO: (upper) before introduction of Zr, and (lower) after Zr doping in the model.*

References

S1 L. Wang, T. Maxisch, G. Ceder, Oxidation energies of transition metal oxides within the GGA+U framework, *Phys. Review B* 2006, **73**, 195107.

S2 L. Wang, T. Maxisch, G. Ceder, A First-Principles Approach to Studying the Thermal Stability of

Oxide Cathode Materials, *Chem. Mater*. 2007, **19**, 543-552.

S3 Y. Kim, J. Kim, S. Kang, First-principles thermodynamic calculations and experimental investigation of Sr–Si–N–O system—synthesis of $Sr_2Si_5N_8$:Eu phosphor, *J. Mater. Chem C* 2013, **1**, 69.

S4 S. P. Ong, L. Wang, B. Kang, G. Ceder, Li-Fe-P-O_2 Phase Diagram from First Principles Calculations, *Chem. Mater*. 2008, **20**, 1798-1807.

S5 P. Shewmon, *Diffusion in Solids*, Springer, Switzerland, 2016.